

# Content Based Medical Image Retrieval Using Clustering Technique

Dr. M. Anline Rejula<sup>1</sup>, Dr. Ben M Jebin<sup>2</sup>, Mr. G. Ravi Selvakumar<sup>3</sup>

<sup>1</sup>Assistant Professor in the Department of Computer Application- P.G, Scott Christian College (Autonomous), Nagercoil, India

<sup>2</sup>Assistant Professor in the Department of Computer Science., Malankara Catholic College, Mariagiri, India

<sup>3</sup>Assistant Professor & Head, Department of Computer Science, Malankara Catholic College, Mariagiri, India

## ABSTRACT

Tumors of the brain are life-threatening and life-defying diseases for humans. For the radiologist, finding a suitable MRI brain tumour picture might be a difficult challenge. Text-based techniques are still the most common method used by most search engines to retrieve pictures. The major issue in MRI image analysis is that the MRI machine captures low-level visual information and the assessor identifies high-level data. To bridge this conceptual chasm, researchers in this study devised a brand-new feature extraction method. CBMIR (Content-Based Medical Image Retrieval) is a new approach to finding pictures of brain tumours in vast databases. MRI pictures are first cleaned up by using a variety of filtering procedures. This is followed by the construction of an algorithm for extracting representative features from MRI images using the Gabor filtering approach and the Walsh-Hadamard transform (WHT) technique, both of which concentrate on a certain frequency content at a specific area of the picture. Using Fuzzy C-Means clustering Minkowski distance metrics, we can then get the most accurate and dependable picture by comparing our query image to a database of photos. Brain tumour MRI images were used to evaluate the suggested technique design. Experiments on brain tumour detection using our suggested method show that it outperforms most of the current methods including Gabor, wavelet, and Hough transform. For radiologists and technicians, the suggested technique will help to construct an automated decision support system that will deliver repeatable and objective outcomes with high accuracy.

Keywords: CBMIR (Content-Based Medical Image Retrieval), Walsh-Hadamard transform (WHT), Magnetic resonance imaging(MRI)

## Article Info

Volume 9, Issue 4

Page Number : 446-459

## Publication Issue :

July-August-2022

## Article History

Accepted : 10 August 2022

Published: 27 August 2022

## I. INTRODUCTION

Among children and individuals under 40, brain tumours are the leading cause of death. When a mass of abnormal cells begins to proliferate and spread throughout the brain, it is considered a tumour. Headaches, visual issues, seizures, memory loss, changes in personality, trouble in concentration, loss of coordination and changes in speech, loss of balance, and mood swings are just some of the physical symptoms that people with a brain tumour suffer. Cancerous (malignant) and noncancerous brain tumours are both forms (benign). Cancerous brain tumours develop more rapidly and infiltrate surrounding tissue than benign ones. When tumours develop, the pressure within the skull might rise. This is true for both benign and malignant tumours. Brain injury, which is life-threatening, may result from this. A patient's quality of life is significantly impacted by brain tumours, and their loved ones must adjust to this new normal. According to the American Cancer Society, the number of Americans who will succumb to malignancies of the brain and spinal cord in 2021 will be about 18,600 [1].

The most common method of identifying a brain tumour is via the use of MRI. MRI provides a wealth of information on the structure of the brain, spinal cord, and arteries. The axial, sagittal, and coronal orientations of these three images will be shown. It is common to use T1- and T2-weighted MRI sequences, as well as Flair (Fluid Attenuated Inversion Recovery). Three-dimensional (3-D) visualisation of anatomical structure is possible using T1 weighted brain images in all three planes: axial, coronal, and sagittal. From the neck to the head, the axial orientation of the MRI head picture is examined. Starting at the point of the nose, the coronal orientation extends back behind the head. From ear to ear, the sagittal alignment is in place. Medical imaging technologies such as CT, MRI, ultrasound, and positron emission tomography (PET) are non-destructive in their approach. As a result, they aid in the acquisition of pictures of organ interiors.

Research on brain image retrieval using Content-Based Image Retrieval (CBIR) has focused on two basic ideas. One kind of technology focuses on automatically extracting pictures from PACS-like databases, which search images of the same imaging modality, body orientation and body area. Another kind of technique focuses on obtaining photos of comparable diseases that are easy to compare for diagnostic purposes. Radiologists face a tough and time-consuming process when attempting to retrieve MRI images from a large collection of similar-structured images. For this method to work, the radiologists must have access to and be able to comprehend MR pictures and be able to retrieve relevant images from the stored data. For a large amount of stored material, this human retrieval method is inefficient, nonreproducible, and time-consuming.

CBIR is a possible approach for indexing historical pictures without the need for radiologists' participation. The retrieval of pictures of brain tumours is the subject of this study, which utilises CBIR. When a radiologist submits a query picture, the CBIR system searches the database for images of the same pathological kind of brain tumour. The radiologist then picks the most closely connected photos that are relevant to the present case's diagnosis and treatment. Over 120 different types of brain tumours have been identified by the WHO, including astrocytoma, gliomas, meningioma, medullo blastoma, and many more. Tumors are divided into three types depending on three factors: their location, grade, and the kind of cells that make up the tumour. Glioma is a specialty in the medical field since it is a common malignancy among adults. When it comes to the treatment of glioma, it depends on its form, location, and size.

A content-based method for obtaining MR images of Glioma brain tumours was developed in this study. Based on the information in the images, the system develops visual characteristics that reflect the content of the picture. To reduce noise, we use many filtering approaches, including Mean Filter, Median Filter,

Conservative Filter, and Crimmins Speckle Removal, and then use the Gabor Walsh-Hadamard Transform strategy to extract features. Last but not least, we use Fuzzy C means with Minkowski to calculate similarity distances between the collected characteristics and an accurately identified brain tumour. Data from a publicly accessible CE-MRI dataset, the entire brain atlas, and other services like IBSR are used to test the method's effectiveness. On the same dataset, we tested robustness, assessed the suggested method's performance, and compared our findings to those of other researchers working on glioma brain tumour picture retrieval.

### 1.1. Need for Brain Portion Extraction

The extraction of the brain component from MR Head scans is a crucial step in numerous image processing and analysis fields, such as image registration, image segmentation and image compression (Atkins and Mackiewich, 1998). In future phases of the tool, the processing time is greatly reduced since the brain's surrounding areas may be disregarded. An important topic of research in medical diagnostics and prognosis is the removal of non-brain areas such as the scalp (bone), skull (fat), eyes, and neck from MR head images (Atkins and Mackiewich, 1998). Skull-Stripping / Brain Extraction is a common term for this technique.

### 1.2. Image Segmentation

Tissue classification is another name for image segmentation, which is the process of identifying distinct kinds of tissue in an MRI scan. Grey matter (GM), white matter (WM), and cerebral spinal fluid (CSF) are the three major brain tissues that are segmented by the brain extraction technique used (CSF). Some of these tissues, such as skin, bone, muscle, fat, and dura, have signal intensities that overlap with those of various other tissues in the brain. This causes an artefact in the strength of the overlap and makes it difficult to accurately identify tissue sections and features. A segmentation or a classification or a clustering algorithm's speed may be correlated to the

number of tissue types or areas it segments. Because of this, it is necessary to first separate the brain in MR images before conducting the brain tissue segmentation technique. GM, WM, and CSF segmentation of head scans is beneficial for a variety of applications, including the identification of cancers, lesions, and multiple sclerosis (MS) (Atkins and Mackiewich, 1998; Clark et al., 1998; Fennema-Notestine et al., 2006; Hartley et al., 2006; Khotanlou, 2009; Smith, 2002).

## II. MRI Principles

Nuclear magnetic resonance is the underlying basis of MRI (NMR). Raymond Damadian and Paul Lauterbur were the first to show the use of NMR for medical imaging in 1971 and 1973, respectively. In NMR, magnetic systems have both a magnetic moment and an angular moment. There are atoms in everything. The nuclei of atoms are made up of protons, neutrons, or a mixture of both. A nuclear spin and a magnetic moment may be found in nuclei with odd numbers of protons, neutrons, or both. The nuclei of most materials, such as  $^1\text{H}$ ,  $^2\text{H}$ ,  $^{13}\text{C}$ ,  $^{31}\text{Na}$ , and  $^{31}\text{P}$ , have magnetic moments (Dhawan, 2003).

The nucleus is formed by the union of protons and neutrons with spins that are in opposition to one another. Since there are equal numbers of protons and neutrons in nuclei with an even number of protons and neutrons, there is no net spin. Because hydrogen has just one proton in its nucleus and hence has a net spin, its nucleus has an NMR signal. Fat and water, both of which have a high concentration of hydrogen atoms, make up the bulk of the human body. The hydrogen nuclei in the bodily tissues are the primary source of the NMR signal for medical MRI.

As the nucleus rotates around its axis, an angular moment is created. Due to its positive charge, the proton creates an axis-defying current loop. A magnetic field is created as a result of the current flowing through it. The magnetic dipole moment of

the proton is formed by the combination of the angular momentum and the self-generated magnetic field. In normal circumstances, there will be no net magnetic field generated by the volume, since the magnetic dipole moments are orientated at random in the material.

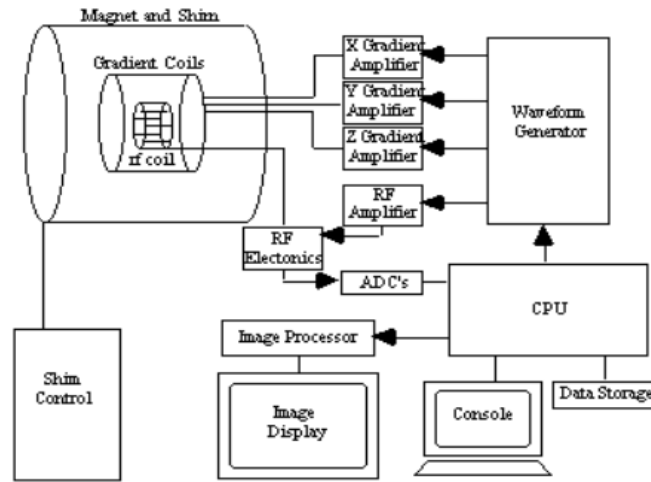


Figure 1.1: A schematic representation of MRI system (Clare, 2006)

Fig.1.1 depicts the key components of a magnetic resonance imaging system. The  $B_0$  imaging field is generated by the magnet. The gradient coils for creating a gradient in  $B_0$  in the X, Y, and Z axes are located inside the magnet. The RF coil is housed inside the gradient coils. In order to rotate the spins through  $90^\circ$ ,  $180^\circ$ , or any other number determined by the pulse sequence the RF coil creates the  $B_{rf}$  magnetic field required. The RF coil also picks up signals from the body's internal spinning. A computerised patient table guides the patient within the magnet's confines. An accuracy of one millimetre may be achieved with this table. A radio frequency (RF) barrier surrounds the scan chamber. Radiation from high-power RF pulses is prevented by the shield. It also shields the 24 imager from the numerous RF frequencies broadcast by television and radio stations. A magnetic shield surrounds certain scan rooms to prevent the magnetic field from leaking out into the rest of the facility. As technology has progressed, the magnet shield has become a fully integrated component of the magnet. At its core, an imager is a computerised device. All of the imager's components are under its command. It is the computer that directs the radio frequency source and pulse programmer, both of which are electronic devices. The source generates a sine wave with the required frequency output. In order to create apodized sine waves, the pulse programmer is used. From milliwatts to kilowatts, the pulse power is increased by the RF amplifier. An additional computer-controlled device is used to adjust the form and amplitude for each gradient pulse. The gradient amplifier boosts the gradient pulses' power so that they can drive the gradient coils' current. A two-dimensional Fourier transform may be performed in a fraction of a second by the image processor on certain imagers.

A pulse sequence is a series of RF pulses used to generate a certain kind of NMR signal (Hornak, 2008). There are a variety of imaging pulse sequences to choose from. SE, inversion recovery (IR), and gradient recalled echo are some of the most often used MRI sequences (GRE). Most people utilise the SE sequence for their pulses since it is the most prevalent. Slice-selective  $90^\circ$ -degree pulses, followed by one or more  $180^\circ$ -degree refocusing pulses, are part of every SE sequence (Ballinger, 2009). In SE sequence, the TR and TE are the two most important variables to consider. When TR and TE are chosen, it has an impact on the overall picture contrast. The addition of T2 dependency to the signal is a benefit of this approach. A T2 dependent imaging sequence is beneficial since

various tissues and diseases have comparable T1 values but vary in their T2 values (Hornak, 2008). With IR pulse sequences, the T1-weighting may be made more pronounced. A 180-degree RF pulse inverts the magnetization, followed by a 90-degree RF pulse that moves the remaining longitudinal magnetism into the transverse plane, where an RF coil can detect it. This is the fundamental portion of an inversion recovery sequence. In imaging, a 180-degree pulse is used to refocus the signal, similar to the SE sequence. The interval between the first 180-degree pulse and the second 90-degree pulse is known as the inversion period (TI). A benefit of this sequence is that its T1 permits the signal from one component to be nulled. This sequence may be used. Fat suppression may be achieved using the STIR (short TI inversion recovery) sequence, which utilises a short TI to eliminate the fat signal while still preserving water and soft tissue signals. The loss of proton signal during the TI period is one of the drawbacks of this sequence. For longitudinal magnetization to be recovered, the TR duration must be longer than the SE time.

### III. Proposed Work

It is the goal of this project to detect brain tumours using a content-based picture retrieval system. In this proposed work, we provide a novel framework for extracting texture features by combining Gabor Walsh-Hadamard Transforms (GWHT). The distance metric measure is utilised for matching in order to get comparable database pictures of brain tumours to the input query image. Fuzzy Clustering using Minkowski distance is a novel distance metric we propose in this work to measure the distance for the similarity between query and database pictures. The optimization of the prediction system is broken down into three stages, as follows.

Using Mean, Median, Conservative, and Scimmins Speckle Removal, we eliminate noise from the raw MRI dataset in Phase 1 (Pre-processing).

Feature Extraction (Phase 2): Using a variety of feature extraction approaches, including the Gabor Transform, Wavelet Transform, Hough Transform, and a hybrid of the Gabor and WalshHadamard Transform, we attempt to extract important properties of the brain tumour.

Phase 3 (Retrieval of Brain Glioma Tumor Image): Using Fuzzy Clustering with Minkowski Distance, we extract brain tumour pictures from an MRI database. The suggested system's design.

#### An MRI Image Pre-Processing

The goal of pre-processing is to enhance the MRI brain pictures' clarity and quality so that they may be used in future analysis. In this study, we used image denoising to remove the noise from the brain picture, allowing us to go back to the original image. Mean filter, Median filter, Conservative Filter, and Crimmins Speckle Removal were some of the tools we used to achieve this end. Using a single filter to preprocess brain tumour photos is very difficult. In the current study solution, a single filter output has more error characteristics, which results in an incorrect prediction. Multiple preprocessing steps provide reliable noise filtering for increased efficacy. The following subsections go into great depth about each filter.

#### Filtering by Means

An image's noise may be reduced using the mean filter. Mean pixel values are calculated using a  $M \times N$  kernel, which is the sum of the individual pixel values. In order to minimise pixel-to-pixel fluctuation, the mean filter is used. This filter replaces each pixel's value with the average of the values in the neighbourhood where it is located. It is possible for a mean filter to remove unrepresentative pixel values from the surrounding environment. The mean value replaces the intensity value of the centre pixel. As a result, the picture is free of noise and has smooth edges. Any filtered data point may be mathematically represented as the average of the latest  $N$  recorded data points for a filter of length  $N$  as The mean filter may alternatively be thought of as a

convolution of the measured signal with a vector of  $N$  constant coefficients, each equal to  $1/N$ . Open-CV package is used to get a mean filter for the picture while applying this filter in Python. Median Filter results are shown in Fig. 2.2.1

## 2) Median Filter

If you use the median filter, it scans the whole picture using a  $3 \times 3$  matrix and recalculates each pixel's value by simply replacing it with its median value. Because median filter generates a more robust average than the mean filter, it is the primary benefit.

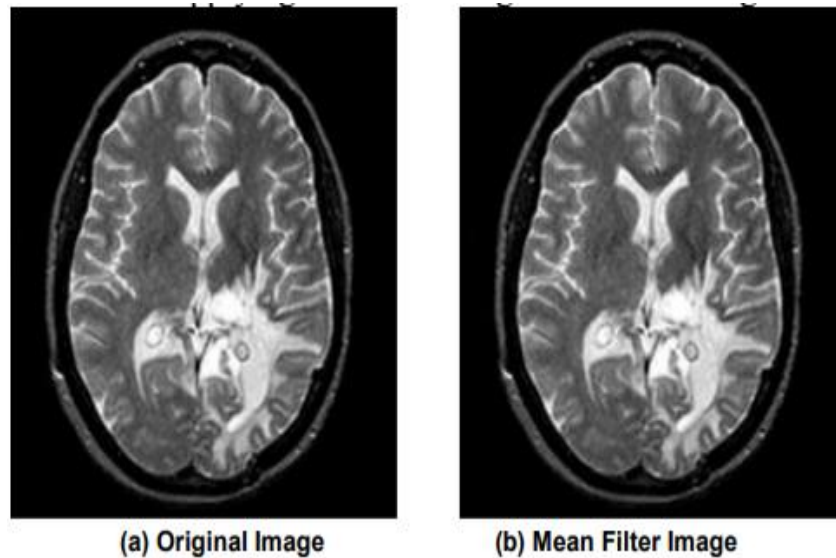


FIGURE 2.1 An example image of Mean Filter

Any pixel value in the vicinity of the neighbouring pixels is considered to be the median. As a result, it will not be able to produce pixels with unrealistic values, which are necessary for pictures to maintain their crisp edges. In terms of brain tumour imaging, this is a very important aspect.

$$X[p, q] = \text{median}\{y[i, j], (i, j) \in Z\}$$

This neighbourhood of pixels is set by the user and centred on a certain place in the picture, which is represented by  $Z$ . Figure 2.2 shows the effect of using a median filter.

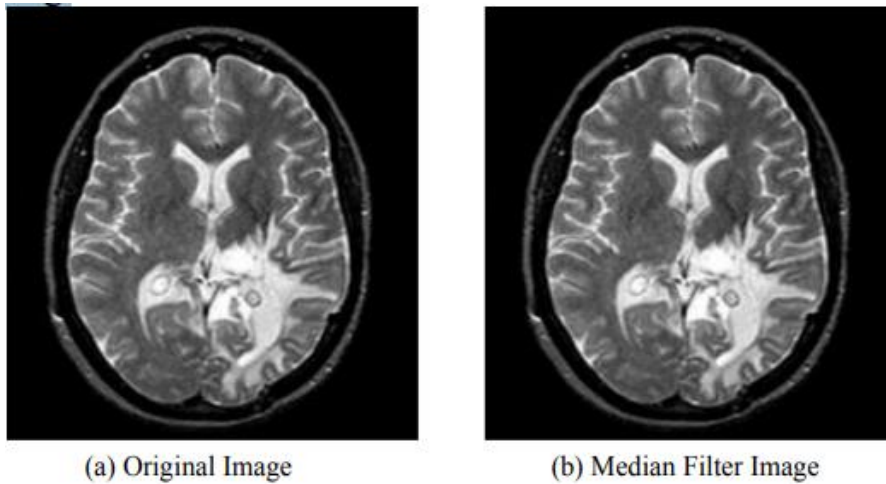


FIGURE 2.2. An example image of Median Filter

1) **Conservative Filter**

The picture may be smoothed and the noise in the image reduced using a cautious smoothing filter. It operates by figuring out the nearest grid cell's lowest and maximum value. Any pixels whose intensity is higher than the computed maximum value are substituted in the final picture with the higher value. The picture should be shown in a window with a resolution of 4 x 4. Take the midpoint of 4 4.

$$out_{img} = \begin{cases} \text{if } mid > max; max \\ \text{if } mid < min; min \end{cases}$$

Similarly, if it is less than the minimum value then it is replaced by the minimum value in the output image. The parameters which are used in conservative filter are neighborhood size, or filter size, is specified in the m and n dimensions. These dimensions should be odd, positive integer values (for example: 3, 5, 7, 9, etc.). Fig. 3.3 shows the resultant of applying the conservative filter.

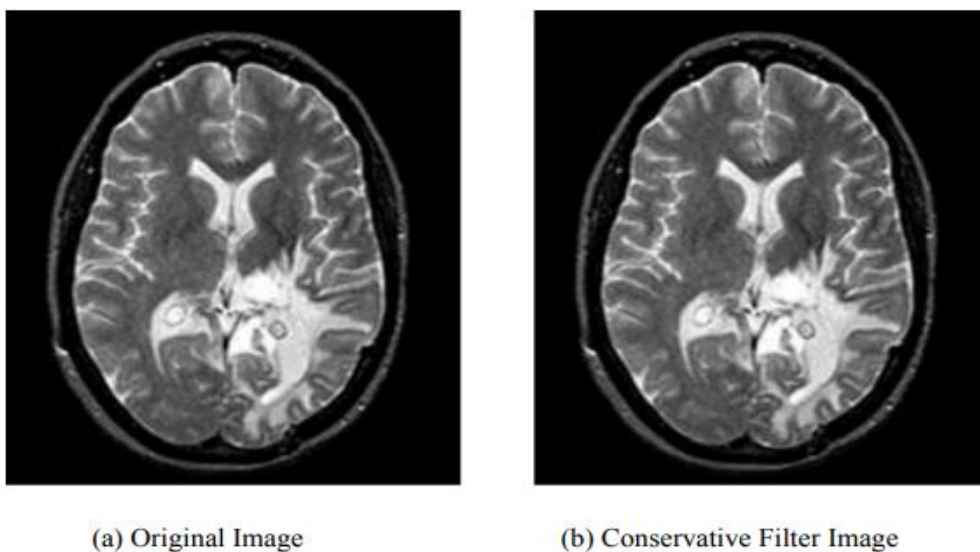


FIGURE 2.3. An example image of Conservative Filter

## 2) Crimmins Speckle Removal

Speckle noise is removed from images using the Crimmins algorithm. The intensity of a pixel in an image is compared to the intensities of its eight neighbours in this technique. Neighbors are considered in four sets by the method (N-S, E-W, NW-SE, NE-SW). P, q, and r are three separate pixels. The algorithm then follows: Follow these instructions for each new iteration.

Each of the four orientations may have its dark pixels adjusted.

1) Apply the following rule to the whole brain image: if  $p > q+2$ , then  $q = q+1$ .

2) Apply the following formula to the whole brain image:  $q = q+ 1$  if  $p > q$  and  $q > r$

If  $r > q$  and  $q > p$ , then  $q = q+ 1$  for the full brain picture. 2) If  $r > q+ 2$ , then  $q=q+ 1$ ; else,  $q=q+ 2$ ;

It allows you to modify the brightness of individual pixels in each of these four directions

If  $p > q > 2$ , then  $q$  is equal to the square root of the square root of  $q+ 1$ .

If  $p > q$  and  $q > r$ , then  $q = q+ 1$  for the full brain picture.

If  $r > q$  and  $q > p$ , then  $q$  Equals  $q+ 1$  for the full brain picture. 4) Apply the following rule to the whole brain image: if  $r > q+ 2$ , then  $q = q+ 1$ . Crimmins Speckle Removal's final product is seen in Figure 2.4.4.

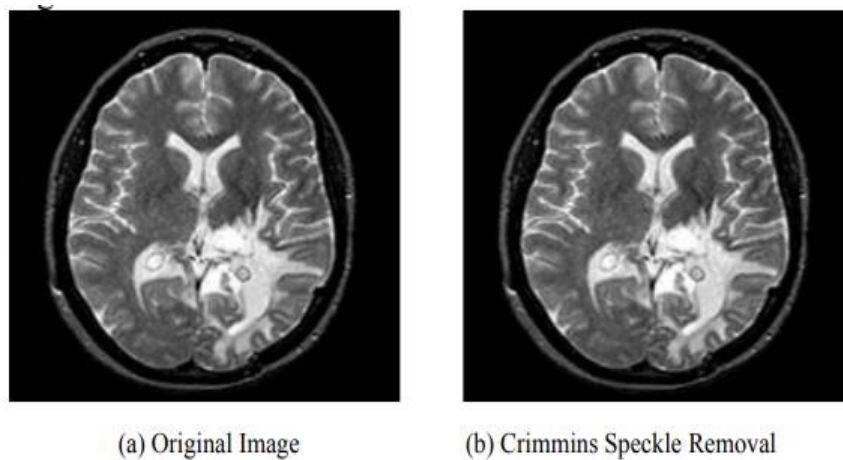


FIGURE 2.4. An example image of Crimmins Speckle Removal

## B. Feature Extraction

The main issue in CBIR is to extract the features which include texture, shape, etc. of the brain image efficiently and then represent them in a particular form to be used effectively in the matching of images. In our proposed work, we implement texture feature extraction by using hybrid of Gabor Walsh-Hadamard Transform (GWHT) technique. Gabor is a multi-scale, multi resolution filter. In Gabor filter pixel value  $x$  and  $y$  denotes the position of the image. Here  $\omega$  denotes center frequency,  $\theta$  denotes the Gabor's orientation of direction and  $\sigma$  shows that standard deviation of Gaussian function with  $x, y$  axis of the image.



$$g(x, y, \sigma) = e^{-\frac{(x-x_0)^2}{2\sigma_x^2} - \frac{(y-y_0)^2}{2\sigma_y^2}} e^{j(\omega_{x0}x + \omega_{y0}y)}$$

Where,

$\omega_{x0}, \omega_{y0}$  – Center frequency of  $x$  and  $y$  directions of the image.

$\sigma_x, \sigma_y$  - standard deviation of the Gaussian function with  $x$  and  $y$  axis or direction.

$x, y$  - Position of the image in pixel format.

Replace the Equation as

$$\varphi(x, y, \omega, \sigma, \theta) = e^{-\frac{(x \cos \theta_k - y \sin \theta_k)^2}{2\sigma_x^2} + \frac{(-x \sin \theta_k - y \cos \theta_k)^2}{2\sigma_y^2}} e^{j(\omega_{x0}x \cos \theta_k + \omega_{y0}y \sin \theta_k)}$$

$$x\theta_k = x \cos(\theta_k) + y \sin(\theta_k)$$

$$y\theta_k = x \sin(\theta_k) + y \cos(\theta_k) .$$

In this work, applied the orientation  $\theta$  of Gabor direction as  $0^\circ, 20^\circ, 40^\circ, 60^\circ, 120^\circ$  with their frequency values of 60, 80, 120, 140. After applying the Gabor Transform to the brain image, the texture features are extracted, in this output applying the Walsh-Hadamard Transform (WHT) to get more accurate and efficient result. WHT is based on correlation between local pixels of the brain image. Walsh transform matrix can be defined as  $WT_i, i = 0, 1, \dots, N - 1$ . The properties of WT are given below:

1. The values of Walsh Transform matrix is(  $WT_i$  ) +1 and -1.
2.  $WT_i[0] = 1$  for all  $i = 0, 1, \dots, N - 1$
3.  $WT_i \times WT_j^T = 0$ , for  $i \neq j$ .
4.  $WT_i \times WT_j^T = N$  for  $i = j$ .

The Walsh transform matrix's row is equal to the row of Hadamard matrix and it is defined by index value of Walsh which is range from 0 to N-1. The Walsh transform matrix's row is equal to the row of Hadamard matrix and it is defined by index value of Walsh which is range from 0 to N-1.

The properties of Hadamard matrix are given below:

1.  $HD_n \cdot HD_n^{-1} = nId_n, Id_n - Identity Matrix$  and

$HD_n$  is the Hadamard matrix.

2.  $|HD_n| = HD_n^{\frac{1}{2n}}$

$$3. HD_n \cdot HD_n^{-1} = HD_n^{-1}HD_n$$

To change the order of Hadamard matrices by permuting rows and columns and also multiplying by the value - 1 in rows and columns. The 4 × 4 matrix is defined as

$$HD_4 = \begin{bmatrix} HD_2 & HD_2 \\ HD_2 & -HD_2 \end{bmatrix} = \begin{bmatrix} 1 & 1 & 1 & 1 \\ 1 & -1 & 1 & -1 \\ 1 & 1 & -1 & -1 \\ 1 & -1 & -1 & 1 \end{bmatrix}$$

Walsh Hadamard Transform (WHT) is defined by sparse factorization of Walsh transform matrix and each factor value is referred as stage. In the WHT the input and output value of each stage is defines as factor value of decomposition. The sparse factorization of identity matrix is obtained from *HD* matrix with its inverse function.

$$HDR^n = Ra^n(HDR^n)^{-1}$$

Where

*HDR<sup>n</sup>* - Walsh Hadamard Transform with radix R

*Ra<sup>n</sup>* - Factorization of radix Ra

n - Number of input element

The WHT consists of Fourier and Cosine Transforms in the basic functions that are a set of orthogonal sinusoidal waveforms. The WHT applied in Squared size gallery space images generating M×M blocks from each image for texture feature extraction. Here we are using 4x 4 blocks. Instead of considering the whole pixels of the image selectively choose the super pixels by using clustering method. These selected pixels are considered as kernel of M×M blocks. The texture features are extracted by projecting sum of selected kernels {*k<sub>0</sub>, k<sub>1</sub>, k<sub>2</sub>, k<sub>3</sub>, … k<sub>15</sub>*} of WHT on the blocks of the image. The diagonal kernels are {*k<sub>0</sub>, k<sub>5</sub>, k<sub>10</sub>, k<sub>15</sub>*}are selected for extracting the texture features of the image.

$$k_0 = \frac{1}{4} \begin{bmatrix} 1 & 1 & 1 & 1 \\ 1 & 1 & 1 & 1 \\ 1 & 1 & 1 & 1 \\ 1 & 1 & 1 & 1 \end{bmatrix}$$

$$k_5 = \frac{1}{4} \begin{bmatrix} 1 & 1 & -1 & -1 \\ 1 & 1 & -1 & -1 \\ -1 & -1 & 1 & 1 \\ -1 & -1 & 1 & 1 \end{bmatrix}$$

$$k_{10} = \frac{1}{4} \begin{bmatrix} 1 & -1 & 1 & 1 \\ -1 & 1 & -1 & 1 \\ -1 & -1 & 1 & 1 \\ 1 & -1 & 1 & -1 \end{bmatrix}$$

$$k_{15} = \frac{1}{4} \begin{bmatrix} 1 & -1 & 1 & -1 \\ 1 & -1 & 1 & -1 \\ 1 & -1 & 1 & -1 \\ 1 & -1 & 1 & -1 \end{bmatrix}$$

To extract the texture feature and gives more clarity to the values by sum of the selected kernel values with projected onto the blocks of the image. These projection of selected kernel values for the blocks of the image is computed as following:

$$\begin{aligned}
 p_1 &= \sum_{i=1}^m b_i * k_0, \\
 p_2 &= \sum_{i=1}^m b_i * k_5, \\
 p_3 &= \sum_{i=1}^m b_i * k_{10}, \\
 p_4 &= \sum_{i=1}^m b_i * k_{15},
 \end{aligned}$$

where  $b_i$  is the  $i^{\text{th}}$  block of the image.  $p_1, p_2, p_3, p_4$  are projection of selected kernels  $\{k_0, k_5, k_{10}, k_{15}\}$  of the blocks of the image. The sum of all projected kernels of the blocks image is calculated as follows:

$$\begin{aligned}
 s &= p_1 + p_2 + p_3 + p_4 \\
 &= \sum_{i=1}^m b_i * k_s,
 \end{aligned}$$

where  $s = 0, 5, 10, 15$  are the diagonal kernel values of the image.

#### Algorithm 1: Gabor and Walsh-Hadamard Transform (GWHT)

Suggestion: a brain tumour discovered through an MRI scan

An option to include texture in the output. The removal of brain tumour tissue

The first step is to read the binary representation of the brain picture from the data collection.

In this step, we use Equation to apply a two-dimensional Gabor filter on the picture.

3rd step: apply the Fourier transform to each block's picture, with a size of 16 x 16. Then choose the Gabor size of 8 x 8 with 5 orientations and 4 scale values from the Fourier converted Gabor picture.

Divide each picture into equal-sized blocks of 4 x 4 using the Walsh-Hadamard transform in step 4.

This specifies how many blocks there are.

Step 5: Using the diagonal kernel values for extracting the texture feature of the picture is the last step in the process.

Project WHT kernels on blocks  $4 \times 4 = \sum_{i=1}^n$

My heart goes out to Nbl i.

$k_n$  represents the  $n^{\text{th}}$  kernel of the block  $bl$ , and  $k_i$  represents the  $i^{\text{th}}$  block  $bl$ .

When calculating the image's texture strength, use the formula  $T = |k_n|^2 - |bl_n|^2$ . For each  $n^{\text{th}}$  block of the  $bl$  picture, the pixel intensity value and the  $k$  denote projected kernel values.

Repeat the steps 6 and 7 for each of the image's blocks to compute the image's texture strength.

A pixel is defined as a block's texture strength multiplied by its number of pixels in the picture.

A Gaussian adjacency matrix A and a Diagonal Matrix D are constructed by taking into account the image's super pixels  $s_1, s_2, s_3, \dots, s_m$  as pixels.

Step 11: Using the Gaussian adjacency matrix A and the diagonal matrix D, construct the Laplacian matrix LM.

Step 12: Denormalize the matrix LM to generate a unit matrix k.

Step 13: Create a cluster for each row of the K-means clustering matrix. When the pixel value closest to the cluster centroid is found, that's where it belongs.

Step 14: Gather all of the K-cluster pixel values.

The pixel values gathered in step 15 are regarded as brain tumour tissues..

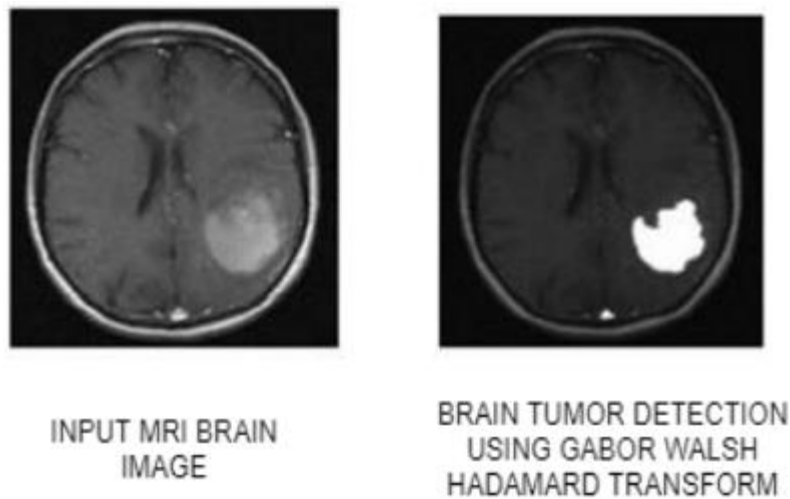


FIGURE 2.5. Result of Proposed Method (GWHT)

### C. Retrieval of Brain Glioma Tumor Image From MRI Database

In this work we used Fuzzy C-Means (FCM) algorithms with Minkowski distance to retrieve the similarity Glioma tumor images from the large image dataset. Main objective of using this algorithm is, it minimizes the Euclidean distance between the data and cluster center. The FCM is stated by:

$$(U, X, \{A_i\}) = \sum_{i=1}^k \sum_{j=1}^N (\mu_{ij})^m D_{ij}^2 A_i,$$

$$\text{Where, } U = [\mu_{i,j}]_{K \times N} \in [0,1]$$

$$X = I^{n \times N}$$

where, U is partition matrix,

$A_i$  is optimization variable used in local norm of matrix, X is set of non-labelled data,

$\mu_{ij}$  is the membership degree of data object  $x^k$  in cluster  $k_i$

$$\mu_{ij} = \frac{1}{\sum_{l=1}^k \frac{d_{ij}^{m-l}}{d_{il}^m}}, i = 1, 2, \dots, k; j = 1, 2, \dots, n$$

Minkowski distance is used.

$$\left(\sum_{i=1}^n |X_i - Y_i|^p\right)^{1/p}.$$

By using Fuzzy C means with Minkowski distance. The most common method for comparing two images in content-based image retrieval is by using an image distance metric measure. For example, a distance of 0 signifies an exact match with the query. The retrieved images are ranked in ascending order based on their relevance.

#### IV. CONCLUSION

Researchers in contemporary image processing have found it difficult to implement content-based picture retrieval. GWHT feature extraction is the basis of our novel CBIR strategy for retrieving brain tumours, which we describe in this study. An improved performance of 97% accuracy is achieved by the suggested approach for obtaining medical images. The examination of the results demonstrates that our suggested method is better to other methods in terms of accuracy and recall. It also required less time to extract features using the suggested technique compared to previous methods of feature extraction. Predicting real positive outcomes as soon as feasible is made easier by retrieving the most recent picture. The problem is that we can't separate out false positive photos if there is a lot of similarity between the pixels in the photographs. The initial stage in medical diagnosis is to find the appropriate picture based on its attributes. It is feasible to anticipate illness onset by using this approach and subsequent processing techniques.

#### V. IMPROVEMENTS FOR THE FUTURE

Some semantic-based similarity computation algorithms may be able to overcome this restriction in the future. The great similarity of pixels in a picture cannot be categorised as a false positive, hence an optimization technique in Artificial intelligence or swarm intelligence may be used to address this constraint.

#### VI. CONCLUSION

The control circuit components are selected to meet established construction and performance requirements. The proposed UL listing standard includes details of such requirements and methods for them to be evaluated. The severest hazard being mitigated by the SIE for connected equipment circuits is electrocution; thus, the overall design requirements

of the SIE device would be for it to achieve the required behavior of safety-related parts to category 4. In order for the internal circuits and components of the SIE device to achieve the safety performance of category 4, they have to be designed so that the following are achieved.

- 1) A single fault in any of the safety-related parts does not lead to a loss of the safety function.
- 2) The single fault is detected at or before the next demand upon the safety functions, such as

immediately, at switch on, or at the end of a machine operating cycle. If this detection is not possible, then an accumulation of faults shall not lead to a loss of the safety function.

3) If the detection of certain faults is not possible, for reasons of technology or circuit engineering, then the occurrence of further faults shall be assumed. In this situation, the accumulation of faults shall not lead to the loss of the safety function. The present designs for the SIE involve circuits and equipment that can be evaluated in a deterministic fashion, and thus, the use of safety performance categories is the present practice. If future systems develop beyond the usefulness of deterministic evaluation, then probabilistic methods would be required.

## VII. REFERENCES

- [1]. Dr.M.Anline Rejula, received her doctoral degree in Computer Applications in 2021, M.Phil.(Computer Science) in 2004, Master of Computer Applications (MCA) in 2002 and Graduation in BSc Mathematics in 1999 from Manonmaniam Sundaranar University, Tirunelveli. She had worked as a faculty member in SSI, Thiruvananthapuram and in a renowned school, Christhu Raja Matric Higher Secondary School, Marthandam. She had more than thirteen years of experience in Noorul Islam College of Arts and Science, Kumaracoil. Now she is working as an Assistant Professor in the Department of Computer Application-P.G Scott Christian College (Autonomous), Nagercoil. In addition to that she has published papers on Image Processing, Deep learning, Network security, Cloud Computing, and books on Relational Database Management System, Internet of Things and Machine Learning using Python.
- [2]. Dr. Ben M Jebin, received his doctoral degree in Computer Applications in 2020, M.Tech(Computer Science) in

2010, M.Phil.(Computer Science) in 2005, Master of Computer Applications (MCA) in 2004 and Graduation in BSc Computer Science in 2001 from Manonmaniam Sundaranar University, Tirunelveli. He had worked as a faculty member for more than 18 years in Trivandrum, Noorul Islam College of Engineering, Kumaracoil, CSI Institute of Technology, Thovalai. Now he is working as an Assistant Professor in the Department of Computer Science., Malankara Catholic College, Mariagiri. In addition to that he has published papers on Image Processing, Neural Network, Deep Learning and Network Security.

- [3]. Mr.G. RAVI SELVAKUMAR received his M.Tech Degree in Computer science in 2007 from Manonmaniam Sundaranar University, Tirunelveli, M.Phil from Manonmaniam Sundaranar university in 2004, MCA from Madurai Kamaraj University in 2002 and B.E Computer Science from Madurai Kamaraj University in 1992. He is working as an Assistant Professor in the Department of Computer Science, Malankara Catholic College, Mariagiri from 1999 with 23 years of teaching experience. His research area is Image Processing

### Cite this article as :

Dr. M. Anline Rejula, Dr. Ben M Jebin, Mr. G. Ravi Selvakumar, "Content Based Medical Image Retrieval Using Clustering Technique", International Journal of Scientific Research in Science, Engineering and Technology (IJSRSET), Online ISSN : 2394-4099, Print ISSN : 2395-1990, Volume 9 Issue 4, pp. 446-459, July-August 2022.

Journal URL : <https://ijsrset.com/IJSRSET229467>